

# Automatic Muscle Artifacts Identification and Removal from Single-Channel EEG Using Wavelet Transform with Meta-heuristically Optimized Non-local Means Filter

Souvik Phadikar<sup>1</sup>, Nidul Sinha<sup>1</sup>, Rajdeep Ghosh<sup>2</sup>

<sup>1</sup>Department of Electrical Engineering, National Institute of Technology Silchar, Assam, India

<sup>2</sup>Department of Information Technology, Gauhati University, Guwahati, India.

## Abstract

Electroencephalogram (EEG) signals may get easily contaminated by muscle artifacts, which may lead to wrong interpretation in the brain-computer interface (BCI) system as well as in various medical diagnoses. The main objective of this paper is to remove muscle artifacts without distorting the information contained in the EEG. A novel multi-stage EEG denoising method is proposed for the first time where wavelet packet decomposition (WPD) is combined with modified non-local means (NLM) algorithm. At first, the artifacted EEG is identified through a pre-trained classifier. Next, the identified EEG signal is decomposed into wavelet coefficients through WPD. Muscle artifacts are eliminated from the wavelet coefficients by estimating the clean wavelet coefficients through a modified NLM algorithm instead of thresholding them. Finally, the artifact-free EEG is reconstructed from corrected wavelet coefficients through inverse WPD. To optimize the filter parameters of the NLM algorithm, two meta-heuristic algorithms, grey wolf optimization (GWO) and particle swarm optimization (PSO), are used in this paper for the first time. The proposed system is first validated on simulated EEG data and then tested on real EEG data. The proposed approach achieved average mutual information (MI) as  $2.9684 \pm 0.7045$  on real EEG data. The result reveals that the proposed system outperforms the recently developed denoising techniques with higher average MI, which indicates that the proposed approach is better in terms of quality of reconstruction and is fully automatic and can be implemented in online applications.

Keywords: Brain-computer interface; Electroencephalogram; EMG; Modified Non-local means filter, Muscle artifacts.

---

## Introduction

BCI is a collaborative setup between the human brain and a computer device, which takes brain signals as input and tries to decode into computer commands to direct external activities such as cursor control, wheel chair control, silent speech recognition, etc. EEG is widely used as a non-invasive way of measuring brain signals in BCI systems due to its high temporal resolutions. It captures the cerebral activities through the electrodes placed over the scalp. EEG is also used in diagnosing several neurological disorders such as Alzheimer's, epileptic seizures, etc. [1]. Generally, BCI records the brain activities, pre-processes them to extract features from the data and finally classifies them for identifying the mental states [2]. Therefore, analyzing the information contained in the EEG is of great importance. Although EEG is intended to record cerebral activities in the form of electrical pulses, but it also captures electrical activities other than the cerebral activities termed as artifacts. EEG signals are widely contaminated with different types of artifact sources such as: cardiogenic (ECG), ocular (EOG), and myographic (EMG). These artifacts suppress the information contained in the EEG signal and lead to wrong interpretation of BCI systems and medical diagnosis. Hence, the elimination of artifacts from the EEG signal is of great importance for practical uses.

The elimination of EMG artifacts from EEG is more challenging as compared to removing other types of artifacts from the EEG signal. Generally, the EMG artifacts occur in EEG signals due to various muscle movement near head. Various muscle movements such as: teeth clenching, swallowing, head movement, chewing, jaw movement, tongue movement, etc. are also captured through electrodes and contaminates the EEG signals with higher amplitude, broad anatomical distribution, and wide frequency spectrum [3]. Specifically, the EMG has a wide spectral band and broad spatial distribution [4]. The power-frequency spectrum of EMG artifacts ranges from 2 Hz to 100 Hz [4]. Their wide spectrum easily overlaps with the frequencies of interest of the EEG. Because

of the influence of both the volume conduction and the broad distribution of muscles across the face, neck, and head, it can be observed anywhere on the scalp.

In contrast, the spatial distribution of ECG and EOG are comparatively localized. EMG artifacts occur from the movement of spatially distributed and functionally independent muscle groups with distinct topographic and spectral signatures [5]. The spectral signatures may vary across different muscles and also with the intensity of muscle contraction. Besides, ECG and EOG artifacts can be removed with the help of a reference channel, while it is difficult to remove EMG artifacts by using reference channels. Due to the complex muscle distribution, the placement of reference electrode for EMG artifact removal is very difficult [5] in a practical situation. Hence, it is challenging to remove EMG artifacts without using any reference channels.

Numerous techniques have been proposed in the literature to overcome these difficulties of EMG removal from EEG. In earlier researches, blind source separation (BSS) based approaches have been explored for the automatic removal of EMG artifact from multichannel EEG [6]. Authors in [7 - 9] showed that independent component analysis (ICA) resulting in a good performance for removing EMG artifacts from the multichannel EEG data. Janani *et al.* [10] showed that canonical correlation analysis (CCA) outperforms the ICA to eliminate EMG from EEG successfully. Chen *et al.* [11] proved that independent vector analysis (IVA) could successfully denoise the EEG signal from EMG. However, BSS-based denoising techniques assume that the number of concerned sources is equal to or less than the number of channels. In this case, BSS can also be implemented for single-channel EEG data [12], where single-channel EEG data was at first decomposed with some decomposition techniques. Then artifactual components from the results of decomposition are used for BSS processing.

However, the recent trend in mobile healthcare applications has led to the reduction in the number of EEG channels for health monitoring and in some cases, only a single channel is used [13]. In such applications, BSS may not perform well. To overcome this issue, several attempts based on the decomposition techniques have been proposed to remove EMG artifacts from few channels and single channel EEG data. Fitzgibbon *et al.* [14] removed EMG artifacts from central channels through the surface Laplacian transform (SLT). They stated that, brain activities captured through central channels are affected only by a group of nonadjacent muscles as there is no muscle under the center of scalp [14] and SLT performed well in removing muscle contamination of scalp signals. However, the neuronal activities from other channels are affected by both the adjacent and the distant group of muscles. Yong *et al.* [15] removed EMG artifacts from both the non-central and distant channels through morphological component analysis (MCA) by assuming that the EEG recordings are linear combination of neuronal activities, artifacts, and electronic noise. However, as the EEG and EMG have non-stationary morphology, the performance of the MCA is not always satisfactory with the chosen dictionaries in MCA. Further, the above-mentioned decomposition techniques are not fully data driven, which make them unfit for automatic and online applications. Bhardwaj *et al.* [16] proposed wavelet transform based EMG artifact removal. The wavelet transform is ideal approach for EEG signal analysis due to its multi-resolution characteristics.

In recent years, several hybrid methods [12, 17 - 27] have been proposed to overcome the difficulties of individual techniques for the removal of EMG artifacts from the EEG data and their summary are shown in table 1. It is observed from the table that EMD based methods have been widely used EMG artifacts correction. However, these methods ignore significant cross-channel interdependence information and consider the dependent information between spatially adjacent channels for the source separation procedure [28]. On the other hand, EMD based techniques perform well on few channel EEG data compared to the single channel EEG data. Whereas wavelet-based techniques perform well on single channel EEG data. The main idea of wavelet-based techniques is to threshold the wavelet coefficients to remove the artifacts from the signal. To threshold the wavelet coefficients, several thresholding techniques such as statistical threshold, and universal threshold calculations are widely used. However, Phadikar *et al.* [29] showed that, these threshold functions may vary with the data which makes the system unfit for automatic and online implementation. Recently, Bajaj *et al.* [30] proposed a tuneable artifact removal technique based on wavelet packet decomposition (WPD). Their denoising method automatically removes EMG artifacts from the corrupted EEG signal. However, the challenge associated with wavelet analysis remains in the selection of proper wavelet function and decomposition level.

Zhang *et al.* [31] proposed convolutional neural network-based approach for the removal of muscle artifacts from the EEG signals. However, their approach is limited for only 2 sec of EEG epoch. A better configuration of CNN is needed for longer duration of EEG. More recently, NLM filter-based methods are employed for the removal of EMG artifacts from the EEG data. Earlier it was designed for image denoising [32]. Eltrass *et al.* [33] proposed a hybrid method where NLM filter is combined with the multi-kernel normalized least mean square with

Table 1: Comparison of recently developed hybrid techniques for the removal of EMG artifacts from the EEG data.

Author(s)	Methodology	Requirement of reference channel	Prior knowledge	Automatic	Online	Can perform on single channel
Mijovic <i>et al.</i> [17]	EEMD-ICA	✗	✗	✗	✗	✓
Sweeney <i>et al.</i> [18]	EEMD-CCA	✗	✗	✗	✗	✓
Chen <i>et al.</i> [19]	EEMD-IVA	✗	✗	✗	✗	✓
Chen <i>et al.</i> [20]	EEMD-MCCA	✗	✗	✗	✗	✓
Chen <i>et al.</i> [12]	MEEMD-CCA	✗	✗	✗	✗	✓
Zeng <i>et al.</i> [21]	MEEMD-ICA	✗	✗	✗	✗	✗
Chen <i>et al.</i> [22]	MEMD-CCA	✗	✗	✗	✗	✗
Xu <i>et al.</i> [23]	MEMD-IVA	✗	✗	✗	✗	✗
Maddirala <i>et al.</i> [24]	SSA-ICA	✗	✗	✗	✗	✓
Dora <i>et al.</i> [25]	Adaptive SSA-NNR	✓	✓	✓	✗	✓
Liu <i>et al.</i> [26]	FEMD-CCA	✗	✗	✗	✗	✗
Li <i>et al.</i> [27]	cICA	✓	✓	✓	✗	✗

EEMD – Ensemble Empirical Mode Decomposition, MCCA – Multiset Canonical Correlation Analysis, MEEMD – Multivariate EEMD, SSA – Singular Spectrum Analysis, NNR – Neural Network Regressor, FEMD – Fast Multivariate Empirical Mode Decomposition, cICA – Constrained ICA.

coherence-based sparsification (MKNLMS-CS) algorithm for the successful removal of the EMG artifacts from the EEG data.

While numerous methods have been studied for the elimination of EMG, developing a robust single or hybrid algorithms which can operate automatically is still very challenging. Also, most of the techniques are suitable for multi-channel EEG (performance degrades for single channel-EEG), hence, developing automatic EMG artifact removal technique for single-channel EEG is still challenging. However, the combination of multiple cascading algorithms is essentially an unexplored area. The significance of cascading algorithms is to suppress the artifacts in a single stage which suppresses artifact sources and achieves higher degree of robustness. In this manuscript, a novel automatic cascaded system is proposed where wavelet transform is combined with the NLM filter for the elimination of EMG artifacts from the EEG signals.

In the proposed work, EMG contaminated EEG signal is automatically identified and decomposed into wavelet coefficients through WPD. Wavelet transform is used to separate the EEG features into different scales so that, significant features of the EEG signals are preserved and noises can be removed. The mother wavelet and appropriate decomposition level is selected through a proper procedure. It is to be noted that, artifacts reflect in the wavelet coefficients. Hence, correcting the corrupted wavelet coefficients will result in denoising EEG signal. In the proposed method, corrupted wavelet coefficients are corrected through optimized NLM algorithm. Finally, all the corrected coefficients are used in inverse operation to get back the original artifact free EEG signal. In this approach, no threshold calculation method is employed; instead, wavelet coefficients are corrected through NLM filter which makes the system automatic and fit for implementation in online applications. In addition, a modified NLM algorithm is proposed, where, all the parameters of the algorithm are optimized in a proper way. The proposed approach preserves the information of interest in the EEG signal which is reflected in higher average correlation coefficients (CC) and higher MI values. The main contributions of the proposed denoising algorithm are stated as:

- 1) The proposed algorithm employs the wavelet transform for its good time-frequency localization, and optimized NLM filter for better removal of wide frequency spectrum EMG artifacts from the corrupted EEG signals.
- 2) The main challenge in wavelet transform based denoising is the selection of appropriate threshold value. Hence, instead of thresholding the wavelet coefficients, they are corrected through NLM estimation.
- 3) The issue of optimum parameter selection for the NLM is properly addressed with the help of meta-heuristic algorithm.
- 4) Further, the proposed algorithm corrects only the EMG corrupted portion of the EEG and keeps the clean portion untouched. Hence, the proposed system preserved the true information contained in the EEG signal.

The novelty of the proposed hybrid method where SVM, WPD and NLM are combined, is described as below:

- SVM is one of the most efficient classifiers and hence, used in this work. Different artifacts have different characteristics such as: eyeblink artifacts contaminate the EEG signals with 5 to 10 times larger amplitude

than the normal EEG signals with very low frequency (typically 0.1 to 3Hz), EMG artifacts contaminate the EEG signals with higher amplitude and higher frequency components. Similarly, ECG artifacts contaminate the EEG signals with periodic discharges. Also, we don't know, which EEG patterns are hidden in the artifacted portions (there is no ground truth). Hence, before removal of artifacts, it is necessary to identify which artifacts contaminate the EEG signals, because different artifacts have different characteristics and affect the EEG signals distinctively. If the system does not have any prior knowledge about the type of artifacts, then the system will be capable of denoising the EEG signals, but the true EEG pattern (or the original ground truth) will not be reconstructed properly. So, first the EEG signals corrupted with EMG artefacts are identified with SVM as a classifier.

- The frequency of muscle artifacts overlaps with the frequency of interest of EEG signals. Hence, removing those particular frequencies by making the relevant wavelet coefficients zero will result in significant loss of information. So, at first EEG signals are decomposed into wavelet coefficients using WPD to represent the different frequency bands of EEG signals with respect to time. Because, designing an efficient NLM based filter for very wide frequency band is very difficult. So, the corrupted EEG signal is decomposed into different frequency bands at different levels in WPD so that efficient NLM filters can be designed for decomposed signals at different levels for the effective removal (correction) of EMG artefacts.
- The optimization of parameters especially the bandwidth parameter,  $\lambda$  of NLM algorithm at different levels (set of  $\lambda$ ) simultaneously is a challenging task and meta-heuristic algorithms are the most efficient ones in solving this type of problems. Hence, one of the recently developed meta-heuristic algorithms, GWO is used for the task.

The manuscript is organized as: Section I introduces the background, state-of-arts, challenges, and objectives, Section II depicts the tools and ideas employed in this methodology, Section III states the proposed methodology, Section IV presents the results, Section V depicts the outcome of the research, Section VI discusses about the experiment, Section VII completes the manuscript by drawing conclusions alongside the strategies for the future works.

## Notations & Preliminaries

Name	Details
$cA_j(k)$	Approximation Coefficients at level $j$ and instant $k$ .
$cD_j(k)$	Detail Coefficients at level $j$ and instant $k$ .
$x(t)$ or $X$	Input EEG signal
$\hat{X}$	Reconstructed clean EEG signal
$Y$	Simulated Corrupted EEG
$y^*$	Simulated clean EEG
$h(k)$	Highpass Filter in Wavelet Packet Decomposition
$g(k)$	Lowpass Filter in Wavelet Packet Decomposition
$d_{ij}$	Wavelet Coefficient at $i^{th}$ level and $j^{th}$ node.
$\hat{d}_{ij}$	Corrected wavelet coefficients
$\epsilon$	Reconstruction Error
$X_{recon}$	Reconstructed signal
$SE_j$	Normalized Shannon Entropy at level $j$
$E_{jk}$	Wavelet Energy Spectrum at level $j$ and instant $k$
$\tilde{u}(s)$	Estimated version of the signal $u$
$N(S)$	Search Neighbourhood
$W(S, \eta)$	Weights corresponding to given sample $S$
$\lambda$	Bandwidth Parameter
$P$	Patch half-width
$M$	Search neighbourhood half-width
$\Delta$	Patch
$L_\Delta$	Number of samples contained in $\Delta$
$d^2(s, t)$	Squared-summation of the point-by-point difference between patches
C-EEG	Corrupted EEG signal
NC-EEG	Non-corrupted EEG signal
$P(,)$	Joint Probability Distribution Function
$P()$	Marginal Probability Distribution Function
SAR	Signal to Artifact Ratio
$W^{-1}$	Inverse WPD Function
$\mu$	Sample Mean
$\sigma$	Standard Deviation
$\sigma_{X^*y^*}$	Cross correlation of the zero mean data $X^*$ and $y^*$

## Materials & Tools

### 2.1 Support Vector Machine (SVM)

The SVM is generally used as a classifier which competently categorizes the data using supervised machine learning algorithm [34]. It creates an optimal hyper plane using the training data to classify the test data. The optimal hyper-plane, also known as support vector creates a decision border from the nearby samples of different data. If the data are linearly inseparable in their original finite dimensions, then, it can be remapped into relatively higher dimensions using kernel tricks. For more details, readers may follow the details described in [35 - 36].

### 2.2 Wavelet Packet Decomposition (WPD)

The wavelet transform decomposes the signals into approximation (cA) and detail (cD) coefficients. cD consists of high frequency information about the signal whereas cA consists of low frequency information. In DWT, after decomposing the signal into cA and cD, only the cA is being decomposed for further higher-level decomposition. To cover the shortage of fixed time-frequency decomposition in DWT, WPD was proposed as an extension of DWT [37]. The WPD not only decomposes the cA but also cD simultaneously. As a result, the WPD has the same frequency bandwidth in each resolution while DWT does not.

For an EEG signal  $x(t)$ , the WPD coefficients can be derived as shown in Eq. (1) [37]:

$$\begin{cases} d_{0,0}(t) = x(t), \\ d_{i,2j-1}(t) = \sqrt{2} \sum_k h(k) d_{i-1,j}(2t - k), \\ d_{i,2j}(t) = \sqrt{2} \sum_k g(k) d_{i-1,j}(2t - k) \end{cases} \quad (1)$$

### 2.3 wavelet Base and Decomposition Level Selection

In the wavelet transform based signal analysis, the selection of the appropriate mother wavelet and decomposition level is a challenging task. Several mother wavelets are available in the wavelet family. The performance of the wavelet transform is affected by individual wavelet function. Since, hit and trial approach is a time-consuming task; the appropriate mother wavelet is selected according to the reconstruction error in this paper. It is to be noted that, when any transformation technique transforms a signal into another domain, and again reconstructs the original signal through inverse operation, the reconstruction error should be ideally zero. The wavelet function is selected which gives the minimum reconstruction error. The reconstruction error ( $\varepsilon$ ) is calculated from Eq. (2):

$$\varepsilon = \sqrt{MSE(X - X_{recon})} \quad (2)$$

The decomposition level is selected through calculating the Shannon entropy (non-normalized) from the wavelet coefficients [38]. Non-normalized Shannon entropy is calculated as shown in Eq. (3):

$$SE_j = \sum_{k=1}^N E_{jk} \log E_{jk} \quad (3)$$

$E_{jk}$  defines as:

$$ED_{jk} = |cD_j(k)|^2 \quad (4)$$

$$EA_{jk} = |cA_j(k)|^2 \quad (5)$$

Since most of the information in the wavelet transformed signals, are stored in the approximation coefficients. Hence, the optimum level of decomposition is selected at which entropy of cA becomes less than that of cD.

### 2.4 Grey Wolf Optimization (GWO)

A swarm-based intelligent algorithm, GWO was first proposed by Mirjalili *et al.* [39], which is followed by the hunting strategy of grey wolves. GWO is a global search-based optimizer, which find the optimum value through mimicking the hunting strategy of grey wolves [40]. Wolves are grouped into four classes say: alpha,

beta, delta, and omega. Alpha is the strongest among the wolves and followed by beta, delta, and omega. The hunting process follow three major steps: searching for prey, encircling the prey, and finally attacking the prey. For more details readers may refer to [39].

## 2.5 NLM Filtering Algorithm

The NLM algorithm drew remarkable attention in image processing. Although it showed promising outcomes in denoising 2D signals or images, it didn't get much attention in 1D signal. In traditional NLM algorithm, at first the 2D image is separated or grouped into distinct regions called patches. Then the denoising is carried out by averaging patches which has similar spatial structure [41]. In similar way, EMG artifacts can be removed from the EEG signals which have a regular repetitive morphology with some variation. However, employing the NLM method for denoising of EEG signal is very challenging because of the non-stationary characteristics of the EEG signals.

Let  $v$  is noisy observation, where,  $u$  is the original signal and  $n$  is the noise then,  $v$  is expressed as in Eq. (6):

$$v = u + n \quad (6)$$

Then, the estimation  $\tilde{u}(s)$  for a given sample  $s$  is calculated by weighted sum of the values at the other point  $\eta$  that are within  $N(s)$ , where,  $N(s)$  is the "search neighbourhood", as described in Eq. (7) & (8) [42].

$$\tilde{u}(s) = \frac{1}{Z(s)} \sum_{\eta \in N(s)} w(s, \eta) v(\eta) \quad (7)$$

$$Z(s) = \sum_{\eta} w(s, \eta) \quad (8)$$

And the weights  $w(s, \eta)$  are expressed as [42]:

$$\begin{aligned} w(s, \eta) &= \exp \left( -\frac{\sum_{\delta \in \Delta} (v(s + \delta) - v(\eta + \delta))^2}{2L_{\Delta}\lambda^2} \right) \\ &\equiv \exp \left( -\frac{d^2(s, \eta)}{2L_{\Delta}\lambda^2} \right) \end{aligned} \quad (9)$$

It is evident from equation (9) that the NLM algorithm extracts the nonlocal information contained in the data. Therefore, the similarity between non local patches is exploited in the NLM technique. It is to be noted that the weights depend upon the patch similarities instead of the gap between them [42]. Hence, averaging over similar patches yields a better estimation of the sample. Subsequently, EEG signal is repetitive in nature, the NLM algorithm may be considered as an effective denoising technique.

The goal of the NLM algorithm is to solve the issues with local smoothing filters by computing the smoothed value as a weighted average of other values in the signal based on the similarity of the neighborhoods. The weights depend on the similarity between blocks/patch. In the NLM algorithm, the similarity between two blocks (patches) is measured in terms of similarity between their neighborhoods as described in the equation (9). The weighting function (exponential as stated in Eq. 9) can be considered as a decaying function based on the similar patches found in the search neighborhood. If the difference between two patches has a large magnitude, then the value of  $w(s, \eta)$  will be small and will have a little effect on output signal. The exponential function decays faster, which leads to set the weight as small value for little bit dissimilar patches, and higher values for similar patches. When the target patches contain muscle artifacts, the algorithm tries to find the other patches similar to the artifacted patches in the search neighborhood. Then, the output signal is estimated by calculating the weighted average of all the similar patches. Finally, the corrected, denoised signal is observed in the output. The novelty of the NLM algorithm is that, the weight  $w(s, \eta)$  depends on the patch similarity, not on the physical distance between samples that means all the parts/patches of the EEG signal which are non-corrupted (similar) will contribute to the new value for a clean part/patch resulting into higher structural similarity. For EMG part with a small number of similar parts/patches are there and hence, the contribution to the weight will be less. Further, averaging will cancel out the all the random noises.

In NLM algorithm, estimation is achieved based on the selected similar patches. The main challenge associated with NLM based EEG denoising is the selection of appropriate filter parameters. There are three key parameters:

bandwidth parameter ( $\lambda$ ), search neighbourhood half-width ( $M$ ), and patch half-width ( $P$ ) that need to be optimized for a better estimation. The value of  $P$  determines the number of patches. The size of  $M$  specifies the area of search, hence, larger the size of  $M$  results in higher computational complexity. Generally,  $M$  is limited to reduce the complexity of the system. Out of the three parameters, selection of appropriate  $\lambda$  is more complicated. The level of the signal's smoothness is determined by the  $\lambda$ . A very small value leads in inadequate averaging, while a very large number can induce signal blurring by causing dissimilar patches to look as identical patches [43]. Generally,  $\lambda$  is calculated as  $0.06\sigma$ ,  $\sigma^2$  is the variance of noise and equal to the 0.002 microvolts [43]. However, only the noisy signal is observed, it is more complicated to estimate the standard deviation of the noise before applying any denoising technique to the corrupted EEG signal. Defining a universal value of  $\lambda$  for EEG signal analysis may be unrealistic as the artifacts that contaminate the EEG signals are not always uniform. A modified NLM algorithm is proposed in this paper, where, the optimum value of  $\lambda$  is selected through meta-heuristic algorithm.

## 2.6 Performance Matrices

To validate and test the proposed method, following parameters are evaluated

2.6.1 Mutual Information (MI): The mutual information measures how much information is drawn from the original corrupted EEG signal to reconstructed clean EEG signal [44]. MI is calculated as in Eq. (10):

$$MI = \iint_{-\infty}^{\infty} P(X, X^{\wedge}) \log \left( \frac{P(X, X^{\wedge})}{P(X)P(X^{\wedge})} \right) dX dX^{\wedge} \quad (10)$$

2.6.2 Average Correlation Coefficient (CC): The average CC computes the degree of similarity between original clean EEG signal and reconstructed clean EEG signal of same duration [44]. The average CC is calculated as in Eq. (11):

$$CC = \frac{C(X^{\wedge}, y^*)}{\sqrt{C(y^*, y^*) * C(X^{\wedge}, X^{\wedge})}} \quad (11)$$

2.6.3 Structure Similarity Index (SSIM): The SSIM calculates the similarity index between original clean EEG signal and reconstructed clean EEG signal of same duration [44]. It is defined as in Eq. (12):

$$SSIM = \left( \frac{2\mu_{X^{\wedge}}\mu_{y^*}}{\mu_{X^{\wedge}}^2 + \mu_{y^*}^2} \right) \times \left( \frac{2\sigma_{X^{\wedge}}\sigma_{y^*}}{\sigma_{X^{\wedge}}^2 + \sigma_{y^*}^2} \right) \times \left( \frac{\sigma_{X^{\wedge}y^*}}{\sigma_{X^{\wedge}}\sigma_{y^*}} \right) \quad (12)$$

The SSIM and average CC are evaluated on simulated EEG data as the ground truth is available. In the case of recorded real EEG dataset, the ground truth is unavailable, hence to determine how much information are preserved from corrupted EEG to reconstructed clean EEG during denoising process, MI is evaluated.

## Experimental Methodology

In this report, a novel hybrid technique for automatic recognition of EMG artifacts and its subsequent elimination from EEG is proposed. The basic flowchart of the proposed algorithm is shown in figure 1. Initially the EEG data is recorded and subsequently processed to remove the artifacts. The stages of the proposed model are as follow:

- Step 1: The corrupted EEG (C-EEG) is identified and separated from the non-corrupted EEG (NC-EEG) with the help of a pre-trained SVM.
- Step 2: The corrupted-EEG is decomposed into wavelet coefficients through WPD using mother wavelet function up to level  $i$  (the mother wavelet and the decomposition level are selected as described in section 2.3).
- Step 3: The wavelet coefficients are then corrected (estimated) through the weighted average of the non-local patches using optimized NLM algorithm. The key parameter ( $\lambda$ ) of the NLM algorithm is optimized using meta-heuristic optimization technique.
- Step 4: Finally, all the corrected wavelet coefficients are reconstructed using the inverse operation to obtain the clean EEG signal.

The different steps of the proposed approach are elaborated in the subsequent section.

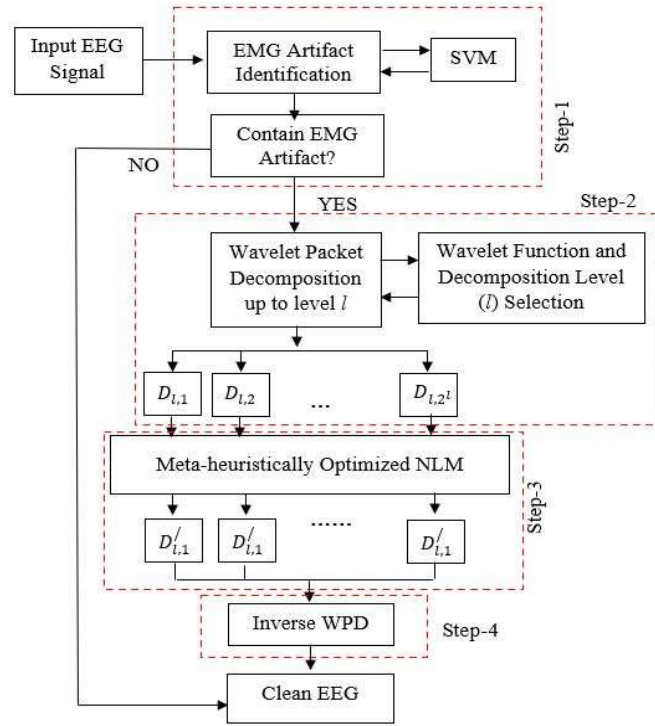


Figure 1: The basic block diagram of the proposed algorithm.



Figure 2: Experimental setup: a subject is performing the various mental tasks.

### 3.1 Data Recording and Processing

Data were recorded from 40 subjects consisting of 26 male and 14 female students (mean age: 21.5 years) to measure the stress of individuals. Ethical clearance has been obtained from the institutional ethics committee and a consent from was signed by individual subjects. The subjects performed various recognition and arithmetic tasks which were selected to elicit short-term stress in students, while their EEG was being recorded. The data were recorded from 32 channels in accordance with the international 10-20 system for placing the electrodes and were sampled at 128 samples per second (1024 Hz internal). The recording was carried out with a wearable 32-channel EMOTIV-EPOC flex gel kit.

The subject is initially asked to relax for a period of 25 seconds where relaxing music is played to ease the subject. The subject is instructed to stay calm after completion of every impulse type. After which, the instructions for the Stroop color and word test (SCWT) is shown to the subjects. The subject is exposed to SCWT for 25 seconds. The subject then relaxes for 5 seconds and then the instructions for the next impulse is displayed for 10 seconds. In the next impulse the subject is shown mirror images and is asked to identify whether the images are symmetric or asymmetric and respond with a thumbs up or thumbs down gesture depending on whether the images



displayed represent symmetric mirror images or not. The mirror image symmetry task is carried out for 25 seconds, after which the subject again relaxes for 5 seconds and then the instructions for the next impulse is displayed for 10 seconds. Finally, the subject is instructed to solve arithmetic problems where the subject is asked to mentally solve the problem and respond with a thumbs up or thumbs down gesture depending on whether the answer displayed on the screen is a correct solution for the arithmetic problem or not. The arithmetic task is also repeated for 25 seconds. The completion of the arithmetic task marks the completion of a trial. Moreover, when the subject is responding, an operator also gives the feedback as to whether the answers provided by the subject are incorrect or correct. The experimental setup is shown in figure 2.

In our experiment, students performed various arithmetic tasks and color tests to measure the stress of individuals. During the experiments it is obvious to move head, shallow or tongue movement etc. which causes the EMG artifacts in the EEG signals. The presence of EMG artifacts in our recorded EEG data are visually inspected by a clinical expert. Generally, normal waveforms of the EEG ranges from 0.1 to 40 Hz. In our experiment, EEG signals are filtered between 0.1 to 40 Hz. to remove the frequency components above 40 Hz.

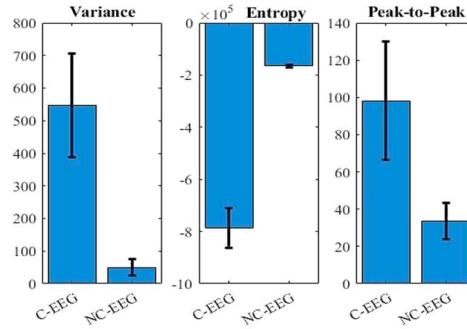


Figure 3: Comparison of the average value of features extracted from C-EEG and NC-EEG.

### 3.2 Identification of C-EEG

From the recorded data clean and corrupted EEG segments were extracted by an expert by studying various parameters like the variance, shannon entropy. Also, the expert visually inspected the EEG for segmenting. A total of 400 segments (duration: 10 sec) were extracted to represent each of the two classes namely: C-EEG and NC-EEG. The SVM network was trained with the features extracted from both the dataset of same size of 10 sec. Three distinctive features: variance, shannon entropy, and peak-to-peak were calculated from all the signals and provided to train the SVM network. To demonstrate their effectiveness in classifying C-EEG from NC-EEG, an SVM network is trained with these features extracted from EEG data of both the dataset. The average values of these extracted features of NC-EEG, and C-EEG are evaluated respectively and showed in figure 3, which demonstrates the extracted features are distinctive between both the classes. The MATLAB function ‘fitcsvm’ was used to train the classifier with default parameters.

### 3.3 Wavelet Decomposition

After successful identification of the EMG corrupted EEG signal, it is passed to the second stage of the proposed algorithm for EMG correction. The C-EEG is decomposed into wavelet coefficients through WPD. Wavelet transform is used to separate the EEG features into different scales so that, significant features of the EEG signals are preserved and noises can be removed. To cover the shortage of fixed time-frequency decomposition in DWT, WPD is employed in the work, which not only decomposes the cA but also cD simultaneously. As a result, the WPD has the same frequency bandwidth in each resolution while DWT does not.

#### 3.3.1 Mother Wavelet and Decomposition Level Selection:

The mother wavelet is carefully chosen by considering the lower reconstruction error as described in the section 2.3. With the minimum reconstruction error, the mother wavelet is selected for decomposing the artifacted signal. Several artifacted EEG signals are analysed using several mother wavelet functions and their average reconstruction error is presented in the table 3. It is observed from the table that, “**fk6**” provides lowest average reconstruction error in analysing EEG signals. As stated in [38], the decomposition level is selected in which the Shannon entropy of cA becomes less than that of the cD. Hence, the artifacted signal is decomposed into wavelet coefficients using “**fk6**” as mother wavelet up to level 5 and their corresponding Shannon entropy values are

compared in table 4. It is evident from the table that, Shannon entropy of cA is less than cD at decomposition level 3. Therefore, in the proposed method, the C-EEG is decomposed into WPD coefficients using “fk6” as mother wavelet up to level 3.

Table 3: Wavelets Vs. Average reconstruction error.

Wavelets	Average $\varepsilon \pm \text{std}$	Wavelets	Average $\varepsilon \pm \text{std}$	Wavelets	Average $\varepsilon \pm \text{std}$
Haar	$4.07\text{e}^{-12} \pm 3.21\text{e}^{-12}$	db11	$3.88\text{e}^{-12} \pm 1.37\text{e}^{-12}$	coif2	$4.45\text{e}^{-10} \pm 1.35\text{e}^{-10}$
db2	$2.62\text{e}^{-11} \pm 7.07\text{e}^{-12}$	db12	$3.81\text{e}^{-12} \pm 1.57\text{e}^{-12}$	coif3	$2.38\text{e}^{-11} \pm 7.33\text{e}^{-12}$
db3	$2.61\text{e}^{-10} \pm 9.00\text{e}^{-11}$	sym2	$2.62\text{e}^{-11} \pm 7.70\text{e}^{-12}$	coif4	$1.10\text{e}^{-09} \pm 3.12\text{e}^{-10}$
db4	$4.91\text{e}^{-11} \pm 1.67\text{e}^{-11}$	sym3	$2.61\text{e}^{-10} \pm 9.0\text{e}^{-11}$	coif5	$2.43\text{e}^{-07} \pm 7.01\text{e}^{-08}$
db5	$7.68\text{e}^{-11} \pm 2.83\text{e}^{-11}$	sym4	$2.29\text{e}^{-11} \pm 6.65\text{e}^{-12}$	fk4	$8.99\text{e}^{-14} \pm 7.67\text{e}^{-14}$
db6	$4.58\text{e}^{-11} \pm 1.77\text{e}^{-11}$	sym5	$8.08\text{e}^{-12} \pm 2.34\text{e}^{-12}$	<b>fk6</b>	<b><math>5.97\text{e}^{-14} \pm 3.26\text{e}^{-14}</math></b>
db7	$6.18\text{e}^{-11} \pm 1.93\text{e}^{-11}$	sym6	$3.57\text{e}^{-11} \pm 1.03\text{e}^{-11}$	fk8	$7.56\text{e}^{-08} \pm 2.19\text{e}^{-08}$
db8	$1.27\text{e}^{-10} \pm 4.50\text{e}^{-11}$	sym7	$3.47\text{e}^{-11} \pm 1.00\text{e}^{-11}$	fk14	$1.12\text{e}^{-10} \pm 3.26\text{e}^{-11}$
db9	$1.38\text{e}^{-09} \pm 4.01\text{e}^{-10}$	sym8	$7.01\text{e}^{-12} \pm 2.50\text{e}^{-12}$	fk18	$7.58\text{e}^{-10} \pm 6.69\text{e}^{-10}$
db10	$1.46\text{e}^{-10} \pm 4.40\text{e}^{-11}$	coif1	$4.23\text{e}^{-11} \pm 1.23\text{e}^{-11}$	fk22	$1.80\text{e}^{-08} \pm 1.18\text{e}^{-08}$

Table 4: Shannon entropy value corresponding to the different decomposition level (mother wavelet: ‘fk6’)

Decomposition level	Shannon Entropy	
	Detail Coefficients	Approximation Coefficients
1	$1.69\text{e}^{+4}$	$3.07\text{e}^{+4}$
2	$1.30\text{e}^{+3}$	$1.69\text{e}^{+2}$
3	<b><math>0.98\text{e}^{+3}</math></b>	<b><math>-1.32\text{e}^{+2}</math></b>
4	786.31	$-1.68\text{e}^{+3}$
5	-409.13	$-3.08\text{e}^{+4}$

### 3.4 Correction of the Wavelet Coefficients

It is to be noted that the EMG artifacts present in the EEG signal will be reflected on its corresponding wavelet coefficients. Hence, correcting them will successfully remove the EMG artifacts from the EEG signal. Now, the artifact free wavelet coefficients are estimated from the artifacted wavelet coefficients using weighted average of the similar patches as described in equation (7). The estimation is performed through NLM algorithm. The selection of the optimum parameter of NLM algorithm is described below.

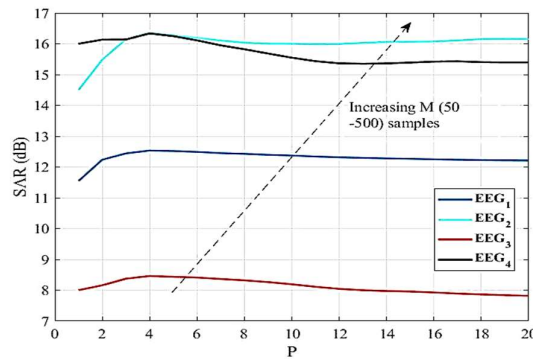


Figure 4: Demonstration of SAR improvement for different values of P at  $\lambda = 0.0469$ . Curves are plotted for different M (50 to 500). The arrow denotes the increasing values of M.

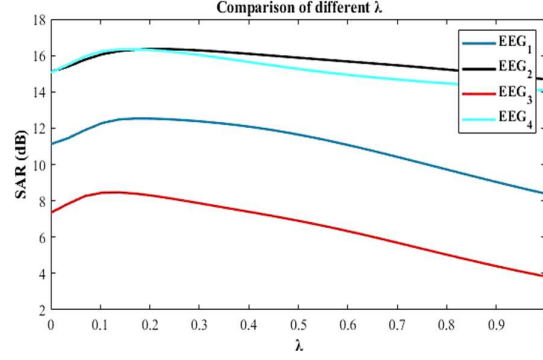


Figure 5: SAR improvements for different values of  $\lambda$  at  $P = 4$  and  $M = 50$ .

An artifacted EEG signal is decomposed into WPD coefficients. All the artifacts will be reflected on WPD coefficients. Then artifact free coefficients are estimated through NLM algorithm by tuning its parameters ( $P$ ,  $M$ ,  $\lambda$ ). Four corrupted EEG signals of duration 10 sec. are analysed by varying the parameters of the NLM algorithm. The SAR improvements achieved by varying several values of  $P$  and  $M$  are shown in figure 4. It is evident from the figure that, SAR varies with the different values of  $P$ . However,  $P = 4$  provides the maximum SAR for different EEG signals. It is also noted that  $M$  does not affect the SAR, but it increases the computational time as shown in table 5. The SAR values for different  $\lambda$  is also compared and shown in figure 5. Unlike  $P$  and  $M$ ,  $\lambda$  is different for different EEG signals yielding the highest SAR. Hence, for NLM based automatic EEG denoising, it is required to optimize the  $\lambda$  to prevent the over smoothing and incorrect patch similarity. Besides, wavelet coefficients at different scales have different characteristics, hence, single  $\lambda$  for all the scales will degrade the smoothness of the EEG signal. In the proposed work,  $2^i$  number of  $\lambda$  are optimized for the  $2^i$  number of wavelet coefficients (where,  $i$  is the decomposition level) through GWO. The selection of appropriate parameters of NLM algorithm is explained in section 3.4.1.

Table 5: Comparison of the computation time for different values of  $M$ .

$M$ (Samples)	Computational Time (Sec.)
$M = 50$	1.8670
$M = 100$	2.7999
$M = 150$	3.7531
$M = 200$	4.6373
$M = 250$	5.4545
$M = 300$	6.5207
$M = 350$	7.2739
$M = 400$	8.0866
$M = 450$	8.8712
$M = 500$	10.4860

#### 3.4.1 Parameter Selection in NLM-based Denoising:

The parameters of NLM algorithm are carefully chosen so that the proposed algorithm gives the best performance for removing EMG artifacts from the EEG signals. In proposed algorithm, several sizes of  $P$  and  $M$  are investigated and their performance in terms of SAR is compared in the above-mentioned figure 4. It is observed from the figure that, the  $P = 4$  performed better in terms of SAR and  $M = 50$  for lower computational time irrespective of the characteristics of EEG signal.

The bandwidth parameter,  $\lambda$  is the most important parameter in NLM algorithm as it decides the degree of smoothness. In the proposed algorithm,  $\lambda$  is selected through meta-heuristic optimization technique as to avoid the over smoothing problem as well as to select the correct similar patches. Two meta-heuristic optimizers, PSO, widely used by researchers due to its fast convergence, and GWO, due to its better execution, are employed for searching the optimal  $\lambda$  for performance comparison.

Let  $x(t)$  be an EEG signal and  $n(t)$  be a muscle artifact, together they formed C-EEG as in Eq. (13):

$$Y = x(t) + n(t) \quad (13)$$

Now, the WPD coefficients  $d_{i,j}$  is extracted from the  $Y$  using “fk6” as mother wavelet up to level  $i$ . Next, corrected WPD coefficients ( $\hat{d}_{i,j}$ ) are estimated from  $d_{i,j}$  using proposed optimized NLM algorithm. The bandwidth parameter  $\lambda_n$  ( $n = 1, 2, \dots, 2^i$ ) is optimized for each coefficient vector. For example, in the proposed method,  $Y$  is decomposed up to level 3 which implies that, eight coefficient vectors are extracted from  $Y$  as  $D_{3,1}, D_{3,2}, \dots, D_{3,8}$ . To remove the EMG artifacts from each coefficient vectors, eight values of  $\lambda$  is optimized in the proposed method. Mathematically  $\hat{d}_{i,j}$  is estimated as in Eq. (14):

$$\hat{d}_{i,j} = f(d_{i,j}, P, M, \lambda_n) \quad (14)$$

Where,  $f(\cdot)$  denotes the NLM function. As suggested in [43], the bandwidth parameter  $\lambda$  is selected as  $0.06\sigma$ , where  $\sigma^2$  is the noise-variance and equal to the 0.002. However, EMG artifacts varies with the muscle contraction, in this case,  $\sigma^2$  may vary. Considering this fact,  $\lambda$  is randomly initialized between 0.01 to 0.9 in the proposed algorithm. The fitness function used for PSO and GWO is stated in Eq. (15) & (16):

$$\text{fitness function} = \max(\text{SAR}) \quad (15)$$

$$\text{SAR}_j = 10 \log_{10} \frac{\text{std}(d_{i,j})}{\text{std}(d_{i,j} - \hat{d}_{i,j})} \quad (16)$$

### 3.4.2 Correction

After estimating the parameters of NLM algorithm, the corrupted wavelet coefficients are corrected through the modified NLM algorithm. In the proposed method,  $P = 4$  and  $M = 50$  is selected through hit and trial approach and the  $\lambda$  is selected through GWO. Next, all the corrected wavelet coefficients are passed to the final stage of the proposed method.

### 3.5 Reconstruction

After successfully estimating the clean wavelet coefficients, all the corrected coefficients are used in inverse WPD to reconstruct the original artefact-free EEG signal. The inverse WPD function is expressed as equation (17). Finally, the artefact-free reconstructed clean EEG signal is provided by the proposed model as output.

$$\hat{X} = W^{-1}(\hat{d}_{i,j}) \quad (17)$$

## Experimental Results

The proposed technique is first tested on simulated EMG artifacted EEG data and then verified on multi-channel real EEG data. The testing is performed on simulated signal as the original clean EEG signal (the ground truth) is known. As a result, it is possible to compare the original EEG signal and its correction after adding EMG artifacts with the original EEG. In this way, using simulated EEG signal, the proposed method is tested.

### 4.1 Test on Single-channel Simulated EEG

The EEG signal is contaminated with EMG artifacts. But the information suppressed by the artifacts is not known (there is no ground truth). Hence, to validate the proposed approach, it is evaluated on simulated C-EEG data where the ground truth is available. The EMG contaminated C-EEG signal is simulated in MATLAB using the method described in [45]. At first, the clean EEG segments of duration 10 sec. are simulated by adding 20 sinusoids together with frequencies selected randomly from 0.1 to 30 Hz with sampling frequency as 250Hz. Next the muscle activities are modelled using random noise bandpass filtered between 5 to 45 Hz. Finally, clean EEG segments and muscle activities are added together to form the C-EEG signal.

Table 6: Performance of the Classifier		
Performance	Classifiers	
	SVM	NBC
Sensitivity	98.31	94.09
Specificity	97.91	91.68
Accuracy	99.01	95.34

The simulated artifactual EEG signal is passed through the pre-trained SVM as classifier. The SVM automatically recognizes C-EEGs through the extracted features. The performance in terms of accuracy,

specificity and sensitivity of the SVM classifier is compared with the Naïve Bias Classifier (NBC) and shown in table 6. It is evident from the table that, the SVM effectively classifies the C-EEG from NC-EEG using extracted features. Next, identified C-EEG signal is decomposed into eight WPD coefficient vectors using “**fk6**” as wavelet function as described above. For estimating clean WPD coefficient vectors, proposed NLM algorithm is applied on eight coefficient vectors. For finding the optimum  $\lambda$ , both the optimizer PSO and GWO are implemented and their performance in term of convergence is presented in figure 6. It is observed from the figure that, GWO attains excellence solution with maximum fitness as compared to PSO. The simulated clean EEG signal and EMG signal is shown in the figure 7 (a) and 7 (b) respectively. By adding them, C-EEG signal is generated and shown in figure 7 (c). EMG artifacts are observed in the time of 0 to 1.3sec, 2 to 4.2sec, and 7.6 to 8.5sec in C-EEG. In figure 7 (d), the corrected EEG signal denoised through the proposed algorithm is shown. It is observed that, the proposed algorithm successfully removes the EMG artifacts from C-EEG while preserving true EEG structure. The power spectral density of C-EEG, clean EEG, and reconstructed EEG is also analysed to verify the proposed algorithm and compared in the fig 8. It is observed that, the proposed denoising algorithm preserves the most of the frequency bands in reconstructed EEG.

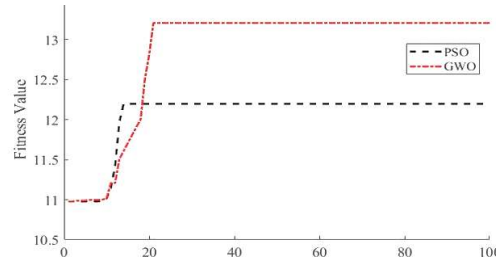


Figure 6: Convergence comparison between PSO and GWO.

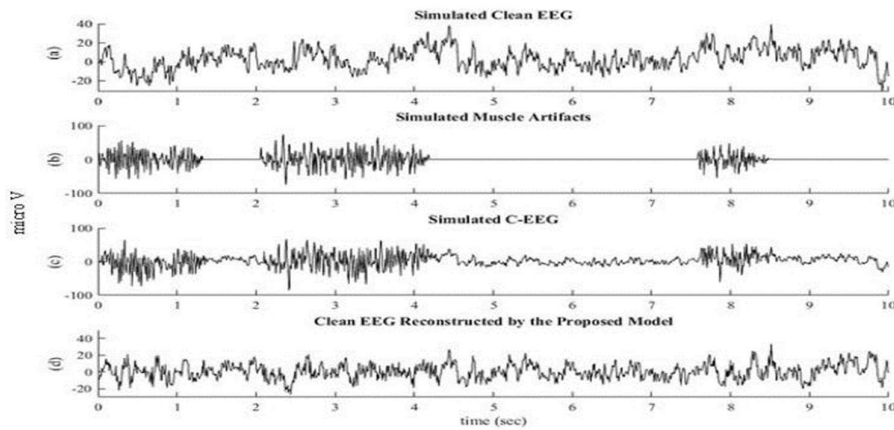


Figure 7: Simulated EEG signal and its corrected EEG signal: (a) Simulated Clean EEG Signal, (b) Simulated EMG Artifact Signal, (c) Simulated Corrupted EEG Signal and (d) Clean EEG Reconstructed by the Proposed model.

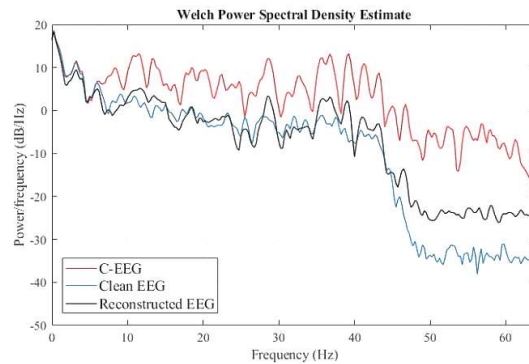


Figure 8: Comparison of Power spectral density among C-EEG, Clean EEG, and Reconstructed EEG.

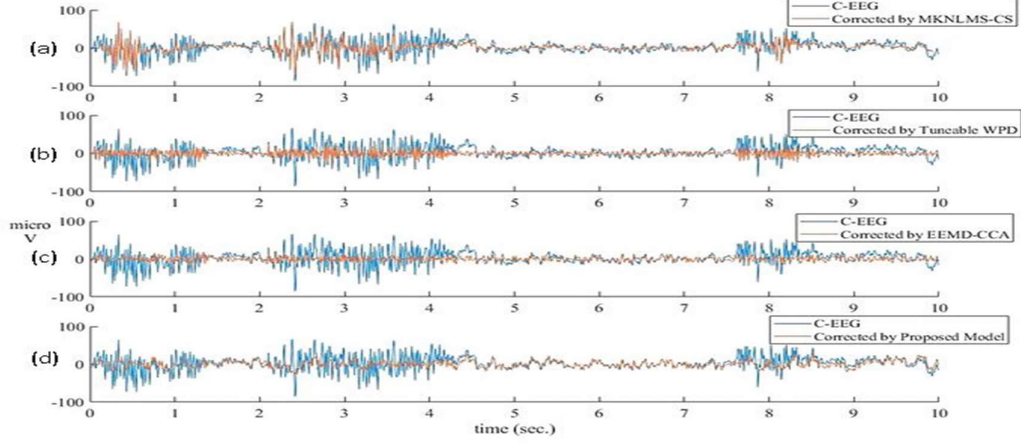


Figure 9: Comparison between simulated corrupted EEG and corresponding clean EEG reconstructed by (a) MKNLMS-CS, (b) Tuneable WPD, (c) EEMD-CCA, and (d) proposed methodology.

To check the superiority, the proposed model is compared with the recently reported EEG denoising techniques [12],[30],[33] and presented in figure 9. In figure 9(a) and 9(b), it is observed that, MKNLMS-CS [33] and tuneable WPD [30] remove muscle artifacts from the C-EEG respectively, while distorting the other portion of the C-EEG where no muscle artifacts are present. EEMD-CCA [12] slightly improves the distortion occurred in the clean portion of the C-EEG as shown in figure 9(c). In figure 9(d) it is observed that the proposed method successfully removes the muscle artifacts while preserving the maximum information contained in the C-EEG. Besides the pictorial evidence, how much information is preserved by all the methods during denoising process is also investigated in quantitative manner. The CC between clean portion of C-EEG and clean portion of reconstructed clean EEG is evaluated to verify how much information is lost during denoising EEG. It is observed from figure 9 that, the EEG portion ranges from 4.3 sec to 7.3 sec does not contain any muscle artifacts. Hence, CC between C-EEG portion (ranges from 4.3sec to 7.3sec) and reconstructed clean EEG portion (ranges from 4.3sec to 7.3sec) is calculated with all the denoising techniques and compared in the table 7. It is evident from the table that the proposed model highly preserves the information contained in the original EEG during denoising the EEG signal. Further, CC and SSIM is calculated between C-EEG and the corrected EEG by all the methods. The performance matrices CC and SSIM are evaluated for all four denoising methods and the proposed method and compared in table 8.

#### 4.2 Test on Multi-channel Recorded EEG Data

After successfully verifying on single channel simulated C-EEG, the proposed model is also tested on recorded EEG. The 32-channel raw EEG data of duration of 10 sec. were chosen from the dataset and filtered between 01 – 40Hz through bandpass filter. However, all the channels are affected by the EMG artifacts. The proposed model automatically recognizes the EMG artifacted EEG data and subsequently corrects them. The proposed model successfully eliminates all the EMG artifacts from corrupted EEG while preserving the true EEG structure. For quantitative analysis, MI between corrupted EEG signal and reconstructed clean EEG is measured and compared with the recently developed techniques as presented in table 9.

Table 7: Comparison of Similarity between C-EEG and reconstructed clean EEG (ranges from 4.3sec to 7.3sec)

Denoising Techniques	Average CC
MKNLMS-CS [33]	0.2809
Tuneable WPD [30]	0.5089
EEMD-CCA [12]	0.5557
Proposed Method	0.8863

Table 8: Performance comparison on simulated C-EEG

Methods	Average CC	SSIM
MKNLMS-CS [33]	0.5937	0.3963
Tuneable WPD [30]	0.7101	0.5401
EEMD-CCA [12]	0.8139	0.5723
Proposed Method	0.8675	0.6809

Table 9: Comparison of MI on 32-channel recorded real EEG data

Channels	MKNLMS-CS [23]	Tuneable WPD [30]	EEMD-CCA [12]	Proposed Method
1	1.009	1.106	2.417	2.970
2	0.952	1.193	2.334	2.972
3	1.562	1.535	2.858	3.985
4	2.389	1.986	3.198	3.908
5	1.410	1.444	2.583	3.207
6	1.053	1.094	2.117	2.652
7	1.119	1.274	2.426	2.958
8	1.630	1.631	2.994	4.179
9	1.930	1.884	2.319	3.010
10	1.427	1.361	3.202	3.359
11	1.601	1.609	2.197	2.387
12	1.198	1.185	2.429	2.798
13	1.039	1.165	2.335	2.842
14	0.932	1.506	2.026	2.127
15	1.109	1.158	2.058	2.199
16	2.011	1.054	2.042	2.292
17	1.520	1.055	2.371	2.747
18	1.106	1.158	2.007	2.446
19	1.321	1.033	2.063	2.496
20	1.030	1.146	1.891	2.305
21	1.098	0.997	2.248	2.451
22	1.032	0.900	2.120	2.421
23	1.001	1.045	2.267	2.691
24	1.030	1.078	2.010	1.985
25	1.131	1.132	1.864	1.783
26	1.095	1.385	2.564	3.289
27	1.521	1.611	3.337	3.914
28	1.302	1.535	2.930	3.181
29	1.015	1.268	2.573	3.151
30	1.400	1.440	2.791	3.465
31	1.612	1.615	3.082	4.607
32	1.590	1.703	2.998	4.211
Average $\pm$ Std	1.3180 $\pm$ 0.3478	1.3214 $\pm$ 0.2747	2.4578 $\pm$ 0.4239	2.9684 $\pm$ 0.7045

## Discussion

In this paper, a fully automatic denoising method is proposed for removing EMG artifacts from the EEG signals. At first, the artifacted EEG signals are identified through SVM as a classifier. After that, the corrupted EEG signals are decomposed into wavelet coefficients through WPD. Wavelet transform is used to separate the EEG features into different scales so that, significant features of the EEG signals are preserved and artifacts can be removed. Generally, in wavelet denoising techniques, wavelet coefficients are thresholded to remove the artifacts. However, selection of appropriate threshold makes the system unfit for automatic operation. In the proposed method, the corrupted wavelet coefficients are corrected through modified NLM algorithm instead of thresholding them. The NLM algorithm has various parameters and needed adjustment for different type of EEG data. A modified NLM algorithm, where the main parameter, the bandwidth parameter is optimized through GWO in this proposed work. In addition, a set of  $\lambda$  is optimized at different scales of the wavelet transformed EEG signal, which enhances the performance of the proposed method for denoising the EEG signals. Finally, all the corrected wavelet coefficients are used in inverse operation to get back the original clean EEG signal. The proposed method is fully automatic and does not need any intervention of the user.

The proposed method is first validated on simulated EEG signals (the ground truth is available) and then tested on recorded EEG data. It is observed from the experimental results, that the proposed method is superior among all the denoising methods in terms of highest CC and SSIM. Hence, the proposed algorithm preserves more true structure of the clean EEG signal compared to other recently reported EEG denoising algorithms. For recorded EEG data, the original true clean EEG is unavailable (there is no ground truth), hence, MI is calculated to check how much information is mutual between corrupted EEG and denoised EEG. It is observed that the proposed approach achieved higher MI as compared to other recently developed techniques.

One of the main advantages of the proposed hybrid method is its insensitive to any threshold value and no need to tune the parameters of NLM algorithm, which makes the system as fully automatic and can be implemented in online applications. WPD efficiently deal with the non-stationary characteristics of EEG signals. Although the proposed method is capable of correcting EMG artifacts from the multi-channel EEG signals, correcting one by one increases the computational time.

## Conclusion and Future Scope

In this paper, a new automatic hybrid system for denoising muscle artifacts from EEG is introduced for the first time, where, WPD is combined with optimized NLM algorithm. The WPD is adopted for its multi-resolution analysis while using only single channel EEG. Unlike other state of art, the proposed system removes artifacts from its time-frequency response of the EEG signal through optimized NLM algorithm instead of thresholding. The proposed system removes the muscle artifacts from EEG signal, no matter how many artifacts contaminate the EEG. Further, several challenges using NLM algorithm for EEG denoising is discussed and properly addressed in this work. One major challenge associated with NLM algorithm is the selection of proper bandwidth parameter. It is also shown that the bandwidth parameter is different for different EEG. In this work, meta-heuristically optimized NLM algorithm is presented, where the bandwidth parameter is selected according to the nature of the EEG. The proposed system can operate automatically and does not require any intervention of the user while using it. The proposed system is first validated with simulated C-EEG, where ground truth is available which demonstrates better performance and then tested with recorded real EEG data for its practical validation. Besides single channel, the proposed system is also able to remove the muscle artifacts from multi-channel EEG data. Future studies are likely to investigate the performance of the proposed method in removing other kinds of artifacts.

## Acknowledgement

The research work is funded by NPIU-MHRD, Government of India, under the CRS Project entitled “Monitoring Stress in Students using EEG”, with CRS-ID: 1-5770264050.

## References

- [1] Ghosh, R., Sinha, N., & Biswas, S. K., 2020. Removal of Eye-Blink Artifact from EEG Using LDA and Pre-trained RBF Neural Network. In *Smart Computing Paradigms: New Progresses and Challenges* (pp. 217-225). Springer, Singapore.
- [2] Phadikar, S., Sinha, N., & Ghosh, R., 2019. A Survey on Feature Extraction Methods for EEG Based Emotion Recognition. In *International Conference on Innovation in Modern Science and Technology* (pp. 31-45). Springer, Cham.
- [3] Shackman, A.J., McMenamin, B.W., Slagter, H.A., Maxwell, J.S., Greischar, L.L. and Davidson, R.J., 2009. Electromyogenic artifacts and electroencephalographic inferences. *Brain topography*, vol. 22, no. 1, pp.7-12.
- [4] Goncharova, I.I., McFarland, D.J., Vaughan, T.M. and Wolpaw, J.R., 2003. EMG contamination of EEG: spectral and topographical characteristics. *Clinical neurophysiology*, vol. 114, no. 9, pp.1580-1593.
- [5] Chen, X., Liu, Q., Tao, W., Li, L., Lee, S., Liu, A., Chen, Q., Cheng, J., McKeown, M.J. and Wang, Z.J., 2019. ReMAE: user-friendly toolbox for removing muscle artifacts from EEG. *IEEE Transactions on Instrumentation and Measurement*, vol. 69, no. 5, pp.2105-2119.
- [6] Mowla, M. R., Ng, S. C., Zilany, M. S., & Paramesran, R., 2015. Artifacts-matched blind source separation and wavelet transform for multichannel EEG denoising. *Biomedical Signal Processing and Control*, vol. 22, pp. 111-118.
- [7] Frölich, L., & Dowding, I., 2018. Removal of muscular artifacts in EEG signals: a comparison of linear decomposition methods. *Brain informatics*, vol. 5, no. 1, pp. 13-22.
- [8] Jiang, X., Bian, G. B., & Tian, Z., 2019. Removal of artifacts from EEG signals: a review. *Sensors*, vol. 19, no. 5, p. 987.
- [9] Chang, C. Y., Hsu, S. H., Pion-Tonachini, L., & Jung, T. P., 2019. Evaluation of artifact subspace reconstruction for automatic artifact components removal in multi-channel EEG recordings. *IEEE Transactions on Biomedical Engineering*, vol. 67, no. 4, pp. 1114-1121.
- [10] Janani, A. S., Grummett, T. S., Lewis, T. W., Fitzgibbon, S. P., Whitham, E. M., DelosAngeles, D., ... & Pope, K. J., 2018. Improved artefact removal from EEG using Canonical Correlation Analysis and spectral slope. *Journal of neuroscience methods*, vol. 298, pp. 1-15.
- [11] Chen, X., Peng, H., Yu, F. and Wang, K., 2017. Independent vector analysis applied to remove muscle artifacts in EEG data. *IEEE Transactions on Instrumentation and Measurement*, vol. 66, no. 7, pp.1770-1779.
- [12] Chen, X., Chen, Q., Zhang, Y. and Wang, Z.J., 2018. A novel EEMD-CCA approach to removing muscle artifacts for pervasive EEG. *IEEE Sensors Journal*, vol. 19, no. 19, pp.8420-8431.
- [13] Minguillon, J., Lopez-Gordo, M.A. and Pelayo, F., 2017. Trends in EEG-BCI for daily-life: Requirements for artifact removal. *Biomedical Signal Processing and Control*, vol. 31, pp.407-418.
- [14] Fitzgibbon, S.P., Lewis, T.W., Powers, D.M., Whitham, E.W., Willoughby, J.O. and Pope, K.J., 2012. Surface laplacian of central scalp electrical signals is insensitive to muscle contamination. *IEEE Transactions on Biomedical Engineering*, vol. 60, no. 1, pp.4-9.
- [15] Yong, X., Ward, R.K. and Birch, G.E., 2009, April. Artifact removal in EEG using morphological component analysis. In *2009 IEEE International Conference on Acoustics, Speech and Signal Processing* (pp. 345-348). IEEE.
- [16] Bhardwaj, S., Jadhav, P., Adapa, B., Acharyya, A., & Naik, G. R., 2015. Online and automated reliable system design to remove blink and muscle artefact in EEG. In *2015 37th Annual International Conference of the IEEE Engineering in Medicine and Biology Society (EMBC)* (pp. 6784-6787). IEEE.
- [17] Mijović, B., De Vos, M., Gligorićević, I., Taelman, J. and Van Huffel, S., 2010. Source separation from single-channel recordings by combining empirical-mode decomposition and independent component analysis. *IEEE transactions on biomedical engineering*, vol. 57, no. 9, pp.2188-2196.
- [18] Sweeney, K.T., McLoone, S.F. and Ward, T.E., 2012. The use of ensemble empirical mode decomposition with canonical correlation analysis as a novel artifact removal technique. *IEEE transactions on biomedical engineering*, vol. 60, no. 1, pp.97-105.



- [19] Chen, X., Liu, A., Peng, H. and Ward, R.K., 2014. A preliminary study of muscular artifact cancellation in single-channel EEG. *Sensors*, vol. 14, no. 10, pp.18370-18389.
- [20] Chen, X., He, C. and Peng, H., 2014. Removal of muscle artifacts from single-channel EEG based on ensemble empirical mode decomposition and multiset canonical correlation analysis. *Journal of Applied Mathematics*, 2014(11).
- [21] Zeng, K., Chen, D., Ouyang, G., Wang, L., Liu, X. and Li, X., 2015. An EEMD-ICA approach to enhancing artifact rejection for noisy multivariate neural data. *IEEE transactions on neural systems and rehabilitation engineering*, vol. 24, no. 6, pp.630-638.
- [22] Chen, X., Xu, X., Liu, A., McKeown, M.J. and Wang, Z.J., 2017. The use of multivariate EMD and CCA for denoising muscle artifacts from few-channel EEG recordings. *IEEE transactions on instrumentation and measurement*, vol. 67, no. 2, pp.359-370.
- [23] Xu, X., Chen, X. and Zhang, Y., 2018. Removal of muscle artefacts from few-channel EEG recordings based on multivariate empirical mode decomposition and independent vector analysis. *Electronics Letters*, vol. 54, no. 14, pp.866-868.
- [24] Maddirala, A.K. and Shaik, R.A., 2017. Separation of sources from single-channel EEG signals using independent component analysis. *IEEE Transactions on Instrumentation and Measurement*, vol. 67, no. 2, pp.382-393.
- [25] Dora, C., Patro, R.N., Rout, S.K., Biswal, P.K. and Biswal, B., 2020. Adaptive SSA Based Muscle Artifact Removal from Single Channel EEG using Neural Network Regressor. *IRBM*.
- [26] Liu, Y., Zhou, Y., Lang, X., Liu, Y., Zheng, Q., Zhang, Y., Jiang, X., Zhang, L., Tang, J. and Dai, Y., 2019. An Efficient and Robust Muscle Artifact Removal Method for Few-Channel EEG. *IEEE Access*, 7, pp.176036-176050.
- [27] Li, Y., Wang, P. T., Vaidya, M. P., Liu, C. Y., Slutsky, M. W., & Do, A. H., 2020. Electromyogram (EMG) Removal by Adding Sources of EMG (ERASE)--A novel ICA-based algorithm for removing myoelectric artifacts from EEG--Part 1. *arXiv preprint arXiv:2007.03130*.
- [28] Chen, X., Xu, X., Liu, A., Lee, S., Chen, X., Zhang, X., McKeown, M.J. and Wang, Z.J., 2019. Removal of muscle artifacts from the EEG: a review and recommendations. *IEEE Sensors Journal*, vol. 19, no. 14, pp.5353-5368.
- [29] Phadikar, S., Sinha, N. and Ghosh, R., 2021. Automatic eye blink artifact removal from eeg signal using wavelet transform with heuristically optimized threshold. *IEEE Journal of Biomedical and Health Informatics*. Vol. 25, no. 2, pp. 475 – 484.
- [30] Bajaj, N., Carrión, J.R., Bellotti, F., Berta, R. and De Gloria, A., 2020. Automatic and tunable algorithm for EEG artifact removal using wavelet decomposition with applications in predictive modeling during auditory tasks. *Biomedical Signal Processing and Control*, vol. 55, p.101624.
- [31] Zhang, H., Wei, C., Zhao, M., Wu, H. and Liu, Q., 2020. A novel convolutional neural network model to remove muscle artifacts from EEG. *arXiv preprint arXiv:2010.11709*.
- [32] Buades, A., Coll, B. and Morel, J.M., 2005. A review of image denoising algorithms, with a new one. *Multiscale Modeling & Simulation*, vol. 4, no. 2, pp.490-530.
- [33] Eltrass, A. S., & Ghanem, N. H. (2021). A new automated multi-stage system of non-local means and multi-kernel adaptive filtering techniques for EEG noise and artifacts suppression. *Journal of Neural Engineering*, vol. 18, no. 3, pp. 036023.
- [34] Ghosh, R., Sinha, N., & Biswas, S. K., 2019. Automated eye blink artefact removal from EEG using support vector machine and autoencoder. *IET Signal Processing*, vol. 13, no. 2, pp. 141-148.
- [35] Cortes, C. and Vapnik, V., 1995. Support-vector networks. *Machine learning*, vol. 20, no. 3, pp.273-297.
- [36] Pisner, D. A., & Schnyer, D. M., 2020. Support vector machine. In *Machine Learning*, Academic Press, pp. 101-121.
- [37] Ting, W., Guo-Zheng, Y., Bang-Hua, Y. and Hong, S., 2008. EEG feature extraction based on wavelet packet decomposition for brain computer interface. *Measurement*, vol. 41, no. 6, pp.618-625.
- [38] Jaffery, Z.A., Ahmad, K. and Sharma, P., 2012. Selection of optimal decomposition level based on entropy for speech denoising using wavelet packet. *Journal of Bioinformatics and Intelligent control*, vol. 1, no. 2, pp.196-202.
- [39] Mirjalili, S., Mirjalili, S.M., and Lewis, A., 2014, Grey wolf optimizer, *Adv.Eng. Softw.*, vol. 69, no. 3, pp. 46–61, 2014.
- [40] Ghosh, R., Sinha, N., Biswas, S. K., & Phadikar, S., 2019. A modified grey wolf optimization based feature selection method from EEG for silent speech classification. *Journal of Information and Optimization Sciences*, vol. 40, no. 8, pp. 1639-1652.
- [41] Van De Ville, D. and Kocher, M., 2009. SURE-based non-local means. *IEEE Signal Processing Letters*, 16(11), pp.973-976.
- [42] Singh, P., Pradhan, G. and Shahnawazuddin, S., 2017. Denoising of ECG signal by non-local estimation of approximation coefficients in DWT. *Biocybernetics and Biomedical Engineering*, vol. 37, no. 3, pp.599-610.
- [43] Ghanem, N.H., Eltrass, A.S. and Ismail, N.H., 2018, June. Investigation of EEG noise and artifact removal by patch-based and kernel adaptive filtering techniques. In *2018 IEEE International Symposium on Medical Measurements and Applications (MeMeA)* (pp. 1-5). IEEE.
- [44] Phadikar, S., Sinha, N. and Ghosh, R., 2020. Automatic EEG eyeblink artefact identification and removal technique using independent component analysis in combination with support vector machines and denoising autoencoder. *IET Signal Processing*, vol. 14, no. 6, pp.396-405.
- [45] Chen, X., Liu, A., Chiang, J., Wang, Z.J., McKeown, M.J. and Ward, R.K., 2016. Removing muscle artifacts from EEG data: Multichannel or single-channel techniques? *IEEE Sensors Journal*, vol. 16, no. 7, pp.1986-1997.